Challenge Journal of Concrete Research Letters

Research Article

Experimental performance analysis of concrete-filled steel column to concrete-filled steel beam connections

Sadrettin Sancıoğlu [a,*], Abdulkerim İlgün [a], Serdar Çarbaş [b]

[a] *Department of Civil Engineering, KTO Karatay University, 42020 Konya, Türkiye*
[b] *Department of Civil Engineering, Karamanoğlu Mehmetbey University, 70200 Karaman, Türkiye*

ABSTRACT

Existing literature and practical engineering practice have comprehensively examined the behaviour of concrete-filled steel tubular (CFST) columns, CFST beams, and their associated connection systems involving either steel or reinforced concrete (RC) beams. Despite these advancements, limited research has focused on the direct beam–column interaction in fully CFST-to-CFST connection configurations. The absence of established design specifications and systematic experimental evidence has hindered the reliable adoption of such connections in structural applications. This feasibility study addresses this knowledge gap by conducting an integrated theoretical and experimental investigation into the structural performance of moment-resisting connections between CFST columns—locally strengthened with internal stiffening plates and configured with external bolted flange connections—and CFST beams of matching geometry. To provide a meaningful benchmark, a comparable hollow steel column–steel beam connection with identical cross-sectional dimensions and bolt arrangements was also evaluated. The experimental setup involved cyclic loading tests designed to capture load–rotation behaviour, quantify flexural stiffness, and identify critical limit states governing connection performance. Detailed measurements of moment–displacement response, local deformation patterns, and strain distribution were collected to assess connection rigidity, load-transfer mechanisms, and potential vulnerability to local buckling. The resulting data allowed for direct comparison between the proposed CFST-to-CFST connection configuration and the hollow steel reference specimen, enabling a clearer understanding of the composite action and confinement effects provided by the infilled concrete. The findings contribute foundational evidence for the feasibility of those moment connections and offer preliminary insights to support future analytical modelling, design recommendations, and full-scale implementation.

ARTICLE INFO

Article history:
Received – September 11, 2025
Revision requested – November 9, 2025
Revision received – November 14, 2025
Accepted – November 24, 2025

Keywords:
Concrete-filled steel tube
Hollow steel tube
Connection
Design code
Experimental analysis

Citation: Sancıoğlu S, İlgün A, Çarbaş S (2025). Experimental performance analysis of concrete-filled steel column to concrete-filled steel beam connections. *Challenge Journal of Concrete Research Letters*, 16(4), 215–224.

1. Introduction

Concrete has considerable compressive strength; however, it demonstrates restricted flexural resistance (Urtekin and Çelik 2025). Conversely, structural steel has enhanced bending capability due to its increased modulus of elasticity. The combination of these two distinct structural elements in a Concrete-Filled Steel Tube (CFST) system facilitates a composite action that proficiently unites the benefits of both materials, yielding enhanced overall structural performance (İlgün and Sancıoğlu 2023). Columns and beams may be implemented with CFST components. Concrete-filled steel elements exhibit a high axial compressive strength due to

* *Corresponding author*. Tel.: +90-444-12-51 ; E-mail address: sadrettin.sancioglu@karatay.edu.tr (S. Sancıoğlu)
ISSN: 2548-0928 / DOI: https://doi.org/10.20528/cjcrl.2025.04.004

the steel's ability to confine the concrete (Yıldız and Şermet 2025; Solak and Orhan 2023). Numerous literature studies have been conducted on concrete-filled steel stub columns to illustrate the cross-section effect and on concrete-filled long steel columns to illustrate the slenderness effect (Kandil et al. 2025; Al-Ani 2018; Ibañez et al. 2018; Liao et al. 2022; Na et al. 2018; Nakanishi et al. 1999; Schneider 1998). Concrete-filled steel beams exhibit a high flexural strength due to the fact that the concrete infill either prevents or delays local buckling. The effects of varying section widths/wall thicknesses, cross-sections, and materials on flexural strength have been demonstrated in literature studies (Abed et al. 2018; Chen et al. 2018; Han et al. 2006; İlgün and Sancıoğlu 2023; Kazemzadeh Azad et al. 2021; Lu and Kennedy 1994).

Recent literature indicates an increase in studies regarding connections between concrete-filled steel columns and steel beams, as well as those between concrete-filled steel columns and reinforced concrete beams. Several of these studies are mentioned as follows; the bolted connection (internal connection) of an H-section steel beam and a concrete-filled steel column was examined by Ye et al. (2021). In the investigation, they implemented two distinct categories of connections. The stiffening rib plate was passed through the column, brought to the opposite face, and welded in the first connection. The flange plates and shear plate were welded to the outside of the box cross-section. The rib plates and shear plates were welded to the column face in the second connection, while the flange plates were passed through the column, brought to the opposite face, and welded. Bolts were the only means of connecting the supports to the column. The investigation was implemented under both monotonic and cyclic loads conditions. The rigidity classification and ductility calculations of the connection were conducted based on the results obtained after monotonic loading, and load-displacement curves were obtained. The energy dissipation capacity of the connection was determined by obtaining moment-rotation curves based on the results obtained after cyclic loading. Wang et al. (2009) conducted an experimental study on a high-strength four-bolt moment-resisting internal beam-column connection subjected to cyclic loading. The study utilized square and rectangular concrete-filled steel columns, as well as H-section steel beams. The variable parameters of the experimental investigation were identified as column section type, column wall thickness, and end plate. The conducted experiments examined the failure mechanism, stiffness, and energy dissipation capacity of the beam-column connection. The experimental investigation determined that the moment-rotation relationship satisfied the essential requirements of international standards, and the strain dissipation and energy dissipation capacities were at the acceptable levels. The findings indicate that the high-strength four-bolt moment-resisting beam-column connection suggested in the study is suitable for application in moment-resisting frame systems. Chen et al. (2014) investigated the seismic performance of a through-beam connection connecting concrete-filled steel tubular (CFST) columns with reinforced concrete (RC) beams. Six specimens were testing under cyclic lateral loading to simulate seismic impacts, subsequently followed by axial compression tests. The findings indicated that the suggested connection had consistent hysteretic behaviour, excellent ductility, and significant energy dissipation capacity. Despite the decrease of stiffness and strength with repeated loading, the overall seismic performance was acceptable. The addition of a reinforcing circular beam adequately reduced the decrease in axial load capacity resulting from the discontinuity of the steel tube at the connection area. Parametric and finite element calculations demonstrated that the reinforcement ratio and axial compressive force significantly impact performance. The study shows that the through-beam connection offers dependable earthquake protection and is applicable in practical engineering with suitable details. Qu et al. (2023) proposed an assembly connection between an H-shaped steel beam and a CFST column and evaluated its seismic behaviour through experiments and finite element modelling. Parametric analyses showed that increasing the end-plate thickness and bolt diameter improves both load-carrying and energy dissipation capacities. The study also demonstrated effective interaction between the connector and concrete, confirming the feasibility of this assembly connection for engineering applications and providing a formula for its bending capacity. Özkılıç (2023) investigated the behaviour of unstiffened extended end-plate connections including thin plates and big bolts by experimental testing and comprehensive numerical analysis. Six specimens performed testing under cyclic and monotonic loads, with end-plate thickness selected as the primary experimental variable to ensure bending-controlled failure. A thorough numerical investigation of 156 finite element models examined the impact of geometric and connection characteristics. The findings indicate that thin end-plates exhibit considerable ductility and strength, although AISC 358-16 and EN1993-1-8 substantially underestimate the plastic moment capacity. Experimental and numerical capabilities exceeded code projections by factors of up to 3.93. A novel yield-line-based formula was introduced, decreasing the real-to-predicted moment capacity ratio to roughly 1.23–1.29, signifying significantly enhanced accuracy. The connections between concrete-filled steel columns and concrete-filled steel beams were investigated by Sancıoğlu (2025) analytically, numerically, and experimentally. Four different connection types were examined within the scope of the study. To enable comparison of moment-carrying performance, the same connection configurations were also tested using hollow steel columns and hollow steel beams. In total, eight specimens—four hollow column–hollow beam connections and four concrete-filled column–concrete-filled beam connections—were subjected to cyclic loading. Based on the experimental data obtained from the cyclic loading tests, the stiffness, moment–rotation behaviour, load–displacement responses, energy dissipation capacity, ductility ratios, performance levels, and failure modes of the connections were evaluated. The performance of each connection type was compared both internally and against the corresponding concrete-filled specimens. Additionally, the experimental results were simulated using the finite element–

based software ABAQUS and compared with the numerical findings. The results demonstrated that the connections composed of concrete-filled steel columns and concrete-filled steel beams exhibited higher load-carrying capacity than their hollow counterparts, achieved the plastic moment capacity specified in the Turkish Steel Structures Regulation (2018), and showed behaviour consistent with the numerical analyses.

As abovementioned in detail, the literature reviews and field applications involve concrete-filled steel columns, concrete-filled steel beams, connections between concrete-filled steel columns and steel beams, and connections between concrete-filled steel columns and reinforced concrete beams. Nonetheless, there are no investigations on the connection between concrete-filled steel columns and concrete-filled steel beams. This pre-study aims to both theoretically and experimentally examine the connection between concrete-filled steel columns with stiffening plates and bolts and concrete-filled steel beams. A hollow steel column-steel beam connection with identical cross-sectional parameters was also examined to compare the concrete-filled steel column and concrete-filled steel beam connections. The experimental investigation provided data for the analysis of moment-displacement curves and the failure modes of the connection.

2. Materials and Method

2.1. Materials

The concrete utilized in the concrete-filled steel columns and beams for the experimental studies was produced in the Structural Mechanics Laboratory of the Civil Engineering Department at KTO Karatay University, according to TS 802 (2016). Three categories of crushed rock aggregates, specifically 0–4 mm, 4–11.2 mm, and 11.2–16 mm, were utilized in concrete manufacturing. Portland cement 42.5 was utilized as the cementing agent. The quantity of additives was designated as 1% of the cement weight. The use of a resin additive resulted in a decrease in both cement and water quantities while preserving the water/cement ratio. Three cubic specimens measuring 150×150×150 mm were extracted from the manufactured concrete for strength evaluation. The specimens underwent water curing for 28 days in a controlled laboratory setting. The cube specimens placed in water for 28 days performed a uniaxial compressive strength test. A uniaxial compressive strength test was performed using a concrete testing press with a capacity of 2000 kN. The test loading rate was established as an average of 0.6 MPa/s, according to the minimum and maximum values specified in TS EN 12390-3 (2019). The mean compressive strength of the concrete specimens was 30.02 MPa. According to Section 12.2.3 of the Turkish Steel Structures Regulation (2018), the compressive strength of concrete used in composite members must fall within the range of 20 MPa to 70 MPa. Therefore, the concrete produced for this study satisfies the specified strength requirements and is deemed suitable for use. The steel cross-sectional dimensions of the columns and beams used in the study were 100×100×3 mm, the column length was 1500 mm, and the beam length was 1000 mm. These dimensions were chosen due to the cost, transportation, and testing difficulties associated with larger column and beam sections. Considering the actual size, the columns are 4500 mm long and the beams are 6000 mm long. Because the internal column-beam joint will be loaded at the centre of the column and the centre of the beam, the test specimens were scaled at a 1:3 ratio. Also, the wall thickness of the connection plates was 5 mm. Three coupon test specimens from each steel group were procured and evaluated according to with TS EN ISO 6892-1 (2020). The structural steel specimens performed tensile testing using a fully automated steel tensile machine with a capacity of 1000 kN. The average yield strength of the structural steel with a wall thickness of 3 mm was 290 MPa, whereas that of the 5 mm wall thickness structural steel was 265 MPa. Additionally, the 8 mm diameter bolts used in the connections had a yield strength of 680 MPa.

In this study, 8.8-grade and 150-mm long bolts were used between the upper and lower surfaces of the columns and beams to ensure load transfer and to address the discontinuity of concrete in the column–beam connection zone. Connection plates and rib plates were also employed in the connections. This connection design, which was originally developed for concrete-filled column–beam joints, was similarly applied to the steel column–beam joints to enable a direct comparison with the hollow steel column–beam connections. Since the established connection type was not previously defined in existing standards or codes, the limitations of the connection were determined based on the relevant criteria outlined in current design standards and regulations. The hole diameters for the M8 bolts used in the study were designed according to Table 13.8 of the principles of design, calculation, and construction of steel structures so-called Turkish Steel Structures Regulation (2018). According to this table, the standard hole diameter for M16 and M24 bolts is set at 2 mm larger than the bolt diameter. However, there is no specific value provided for M8 bolts. Therefore, the diameter of the holes for the M8 bolts was determined as 10 mm. Furthermore, according to Section 13.3.6 of the same regulation, the minimum centre-to-centre distance between standard circular holes, denoted as s, must not be less than three times the nominal bolt diameter, d. Based on this requirement, the minimum bolt spacing for M8 bolts was established as 24 mm. Through this approach, the study ensured that the connection design met the geometric and mechanical requirements defined by national standards, while enabling consistent comparison between different column–beam configurations, including concrete-filled, steel, and hollow steel connections. L-shaped plates were fastened to both the top and bottom flanges of the beam using bolts. Six rib plates were utilized in the L-shaped plates, with three positioned on the bottom and three on the top. The beam was fastened to the column using 12 bolts stretching from the top flange to the bottom flange of the column. The lower flange of the column was reinforced by a supporting connection plate to prevent local buckling during the torque of bolts. Furthermore, six holes

were created on each side of the column and three holes on each side of the beam to help distribute the shear force. Shear plates, extending from the column's lateral surfaces to the beam's lateral surfaces, were fastened to these holes. The connection was established utilizing bolts along the lateral surfaces of the column and beam. Fig. 1 presents specifications of the L-shaped plate connection and dimensions of the L-plate.

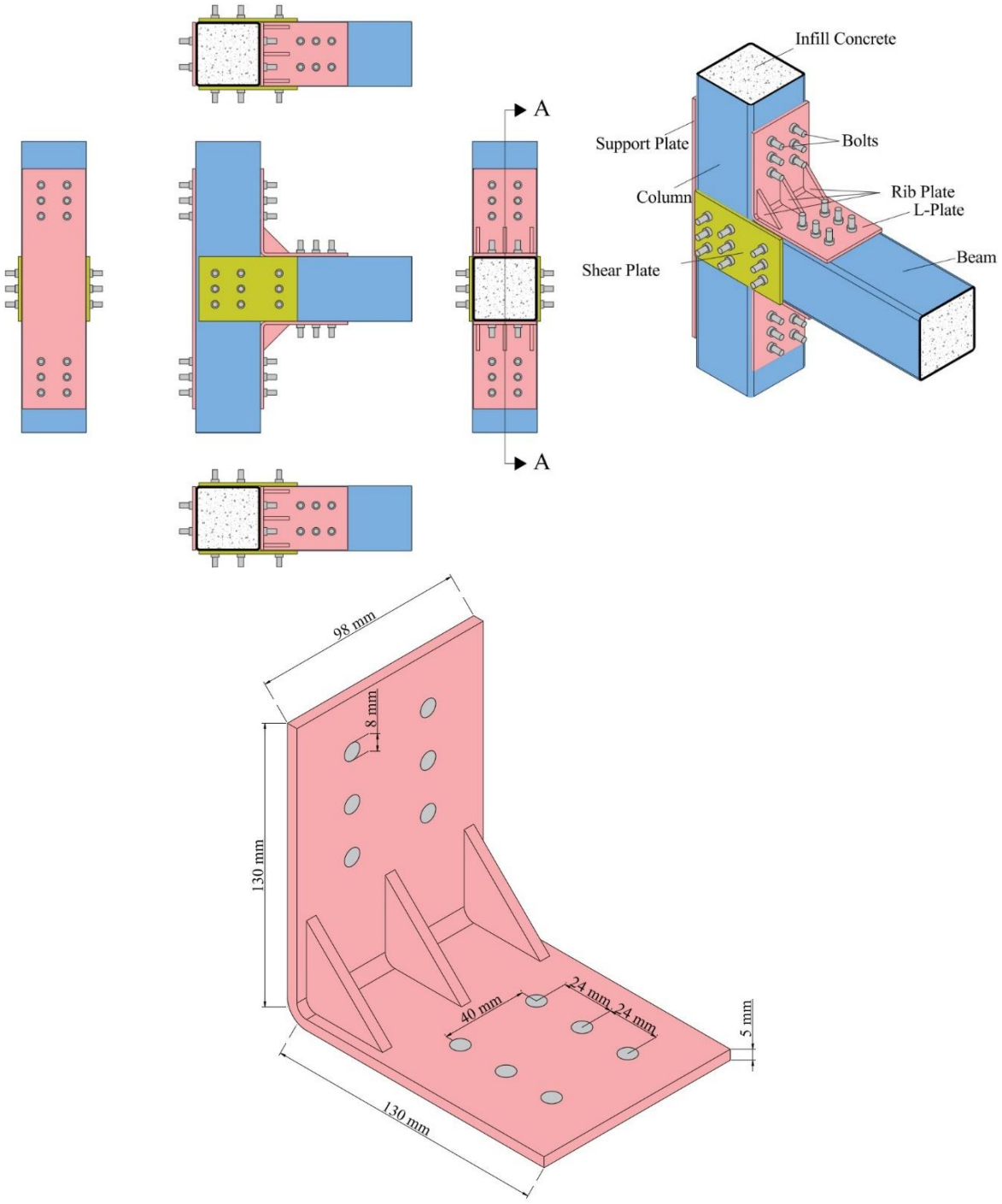

Fig. 1. L-shaped plate connection.

2.2. Method

2.2.1. Theoretical study

A square steel box profile with a cross-sectional property of 100×100×3 mm was selected as the beam section. Thin-walled steel beams must be classified for local buckling according to Turkish Steel Structures Regulation (2018) Section 5.4. The selected beam section is in the compact class. The bending moment strengths for the yield limit states of compact and box-section bending members are calculated according to Turkish Steel Structures Regulation (2018) Section 9.7.1. The bending moment strength for the yield limit state is obtained by multiplying the steel yield strength, F_y, by the plastic moment of strength, W_p. The calculation formula is given in Eq. (1).

$$M_n = M_p W_p \quad (1)$$

A square steel box profile with a cross-sectional property of 100×100×3 mm was selected as the beam section. Concrete-filled steel beams must be classified for local buckling according to Turkish Steel Structures Regulation (2018) Section 12.2.4. Accordingly, the selected beam section is classified as compact. Since the element meets the compact cross-section condition, the characteristic bending moment strength, M_n, was calculated according to Eq. (2).

$$M_n = M_p \quad (2)$$

According to Turkish Steel Structures Regulation (2018) Table 12.4, M_p was calculated according to M_B, where the axial force is taken as zero. M_B is obtained from the interaction diagram developed for composite elements. The calculation formula for M_B is given in Eq. (3). The nominal moment of strength for steel is given in Eq. (4), and for concrete is given in Eq. (5). The location of the neutral axis is given in Eq. (6). The value of the moment at point D in the interaction diagram developed for composite elements is calculated using Eq. (7). The moment of strength of the concrete within the box section is calculated using Eq. (8). To generate moment-displacement graphs, the load and displacement data obtained from the experimental study must be converted into moment and displacement values. Accordingly, moment values, M, were obtained by multiplying the load values given at the beam end, P, by the beam length, L (Fig. 2(c)). The calculation method is given in Eq. (9).

$$M_B = M_D - W_{sn} \cdot F_y - \frac{1}{2} W_{cn}(0.85 \cdot f_{ck}) \quad (3)$$

$$W_{sn} = 2 \cdot t \cdot h_n^2 \quad (4)$$

$$W_{cn} = b_i \cdot h_n^2 \quad (5)$$

$$h_n = \frac{0{,}85 \cdot f_{ck} \cdot A_c}{2[0.85 \cdot f_{ck} \cdot b_i + 4 \cdot t \cdot F_y]} \leq \frac{h_i}{2} \quad (6)$$

$$M_D = W_{px} \cdot F_y + \frac{W_c}{2} W_{cn}(0.85 \cdot f_{ck}) \quad (7)$$

$$W_c = \frac{b_i \cdot h_i^2}{4} - 0.192 \cdot r_i^3 \quad (8)$$

W_{px} = Plastic strength moment of box cross-section according to x-axis

$$M = P \cdot L \quad (9)$$

2.2.2. Experimental study

The experimental setup was established in the Structural Mechanics Laboratory of the Civil Engineering Department of the Faculty of Engineering and Natural Sciences at KTO Karatay University. The experimental setup will utilize hydraulic jacks with 300 and 600 kN load capacities for load application, load cells with 300 and 600 kN capacities for load measurement, linear variable displacement meters (LVDTs) for measuring displacements at column midpoints, beam top endpoint displacements, and beam bottom endpoint displacements. A 2×8-channel static data logger device will be used to collect data during the experiment. The experimental setup is shown in Figs. 2(a) and Fig. 2(b), while the moment-displacement relationship is illustrated in Fig. 2(c).

A review of literature studies reveals that in column-beam connection tests, the columns are subjected to an axial load corresponding to a certain percentage (25–30%) of their axial load-carrying capacity (Ye et al. 2021). In the test, the columns were subjected to an axial load corresponding to approximately 25% of the column's axial load-carrying capacity. This value was approximately 75 kN for hollow specimens and 120 kN for concrete-filled specimens. Cyclic loading was applied using a hydraulic press attached to the beam end. Loading was performed using displacement control according to the values recommended in FEMA-350 Section 3.9.1. The displacement-controlled loading protocol prepared according to FEMA-350 (2000) Section 3.9.1 is shown in Fig. 3.

3. Results and Discussion

3.1. Moment-displacement curves

The cyclic loading test was conducted to investigate the hysteretic behaviour and deformation characteristics of both hollow and concrete-filled beam specimens at their connection regions. During the initial twenty-eight loading cycles, the analysis of moment and displacement values indicated that the connection remained entirely within the elastic range. In this phase, the applied load was fully recoverable upon unloading, and no residual deformation was detected in either the beam or the column. This behaviour confirmed that both materials exhibited a stable elastic response under cyclic loading and unloading conditions. The structural integrity of the connection was thus maintained during the early cycles. After the twenty-eighth cycle, when the displacement reached –30 mm, local buckling was observed in the connection plate. The onset of local buckling occurred as the actuator reversed from the –30 mm displacement, at which point the moment dropped to zero. This sudden loss of load-carrying capacity signified a transition from the elastic to the plastic domain, where the connection began to experience permanent deformation. The formation of local buckling indicated the initiation of instability within the connection plate, which served as the primary locus of inelastic behaviour. Despite this, no permanent deformation was observed in the main body of the beam or column, implying that the damage was localized rather than global. Following the occurrence of local buckling, the moment–displacement behaviour exhibited a clear asymmetry.

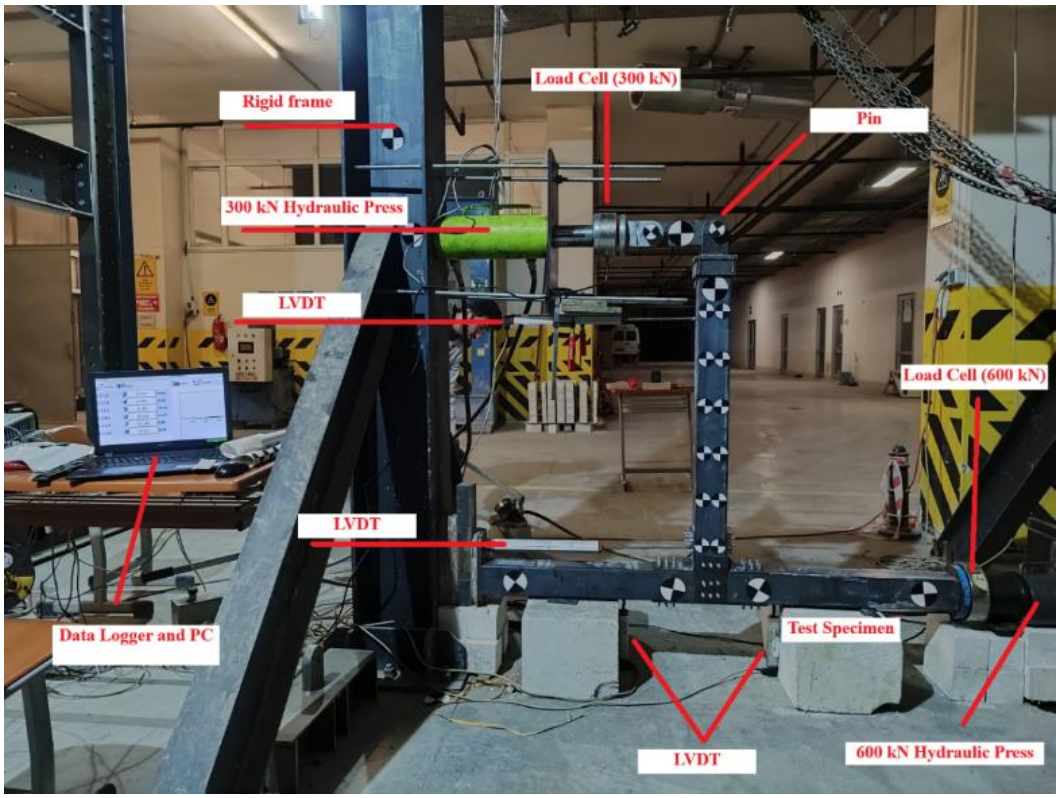

(a) Experimental setup

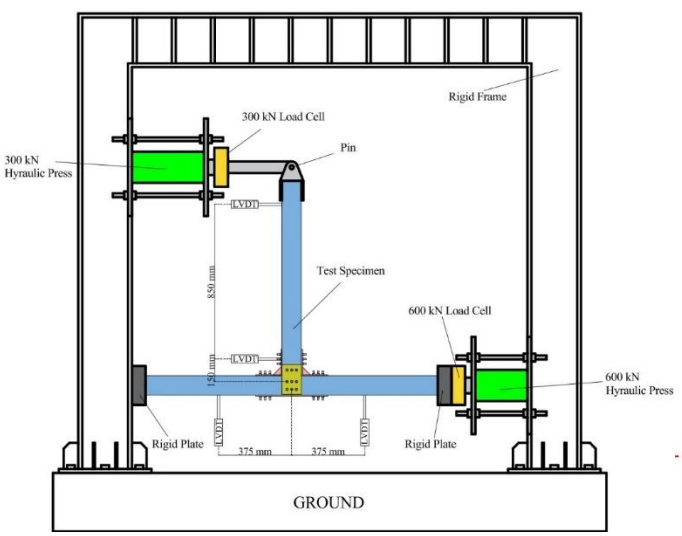

(b) Experimental setup (2D)

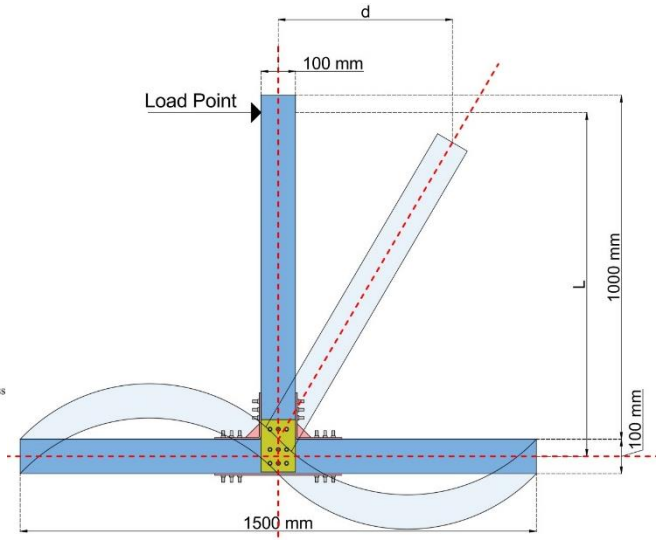

(c) Moment–displacement relationship

Fig. 2. Details of the experimental test setup.

The moments corresponding to equal displacements in the positive and negative directions differed, reflecting the degradation in stiffness and strength in the buckling direction. Such asymmetry is a characteristic feature of cyclic degradation, where the accumulation of plastic strains alters the structural response during subsequent moment reversals. For the hollow specimen, the maximum positive moment was recorded as 3.74 kNm at a displacement of 67.98 mm, while the maximum negative moment reached 5.01 kNm at 68.82 mm displacement. The discrepancy between these values was attributed to local buckling at the connection region, which reduced the moment-carrying capacity in the direction of deformation. This indicates that the hollow section exhibited a progressive stiffness reduction once local instability developed. Nevertheless, no permanent deformation or visible damage was detected in the column or beam, confirming that the failure mechanism was confined to the connection plate. In contrast, the concrete-filled specimen demonstrated a significantly improved performance.

The maximum positive moment reached 6.33 kNm at a displacement of 70.53 mm, and the maximum negative moment was 6.39 kNm at 72.28 mm displacement. The near-symmetry of these values suggests that local buckling in the concrete-filled specimen occurred simultane-

ously in both directions after the maximum moment had been attained. The concrete infill delayed the onset of local buckling and contributed to a more uniform and stable hysteretic response. Moreover, the presence of concrete enhanced the stiffness and energy dissipation capacity of the specimen by providing lateral confinement and delaying instability in the steel plate. When the performance of the two specimens is compared, the concrete-filled beam exhibited a 1.69 times higher moment capacity in the positive direction and 1.28 times higher in the negative direction compared to the hollow specimen (Table 1). This considerable improvement in strength and deformation capacity can be attributed to the composite action between the steel section and the concrete core. The infill effectively stabilized the local plate buckle and increased the ductility of the system under cyclic loading. As illustrated in Fig. 4, the moment–displacement curves of both specimens reveal distinct hysteresis loops. The hollow specimen showed a rapid reduction in stiffness and moment capacity following buckling, whereas the concrete-filled specimen maintained a stable response with wider hysteresis loops, indicating superior energy absorption. These findings confirm that concrete infill plays a critical role in enhancing both the ductility and cyclic load resistance of steel beam connections subjected to repeated lateral loading.

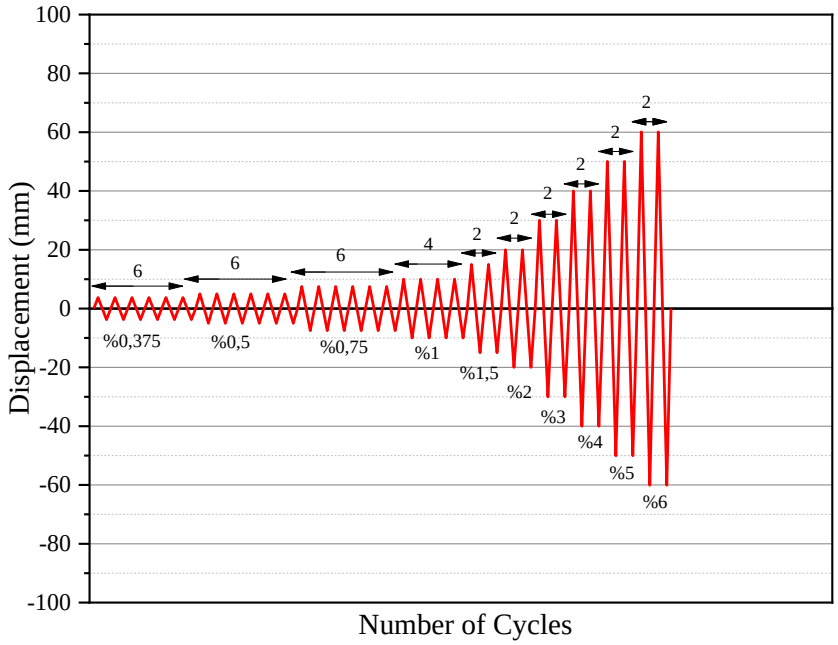

Fig. 3. Displacement-controlled loading protocol.

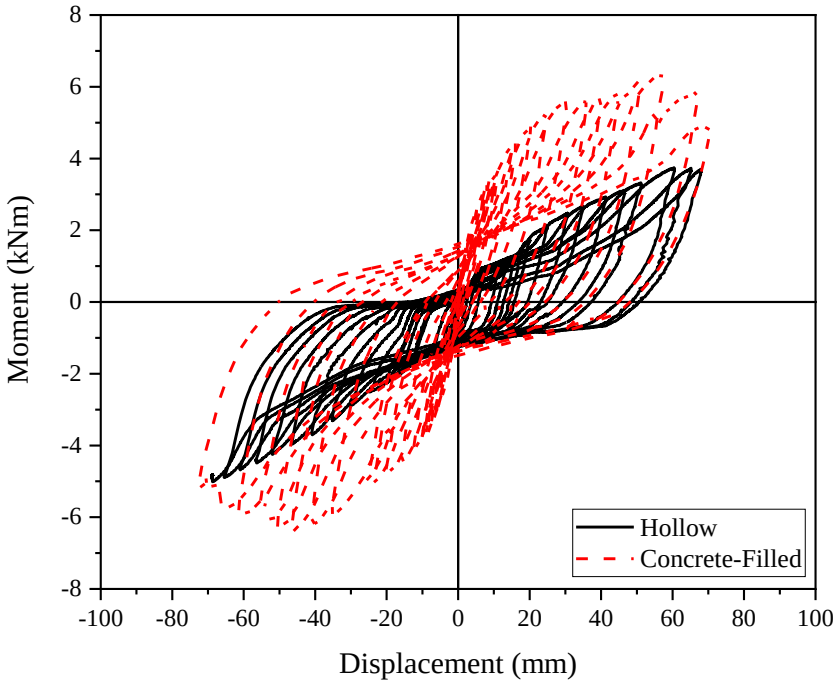

Fig. 4. Moment–displacement curves of the specimens.

Table 1. Comparison between theoretical and experimental results.

	Theoretical results		Experimental results		Experimental / Theoretical	
	Positive maximum moment (kNm)	Negative maximum moment (kNm)	Positive maximum moment (kNm)	Negative maximum moment (kNm)	Positive	Negative
Hollow	11.98	11.98	3.74	5.01	0.31	0.42
Concrete-Filled	13.35	13.35	6.33	6.39	0.47	0.48

3.2. Failure modes

Experimental observations revealed significant local buckling behaviour in both hollow and concrete-filled beam–column connection specimens. In the case of the hollow specimens, local buckling was observed at the connection plates on both the front and back sides of the specimens. This behaviour was primarily attributed to the interaction between the beam and the column during the moment transfer process. As the beam deformed under increasing moment, the column attempted to rotate at the joint, generating localized compressive stresses that exceeded the elastic limit of the connecting plates, thereby initiating local buckling. In the hollow specimens, the onset of local buckling was strongly influenced by the insufficient stiffness of the connection plates and the failure of the bolted joints in the near of the buckled region. These deficiencies caused the plates to lose their elastic response and undergo plastic deformation, significantly reducing the connection stiffness. Consequently, the beam was unable to attain its theoretical moment-bearing capacity, and no local buckling was observed in either the beam or the column members themselves. Instead, the failure was concentrated in the connection region, leading to premature failure before the beam could reach its full moment-carrying capacity.

This observation clearly indicates that the connection stiffness and detailing play a critical role in the overall structural response and moment-transfer efficiency of such assemblies. Conversely, in the concrete-filled specimens, local buckling was again observed in the connection plates at both the front and back sides. The mechanism of buckling formation was similar to that in the hollow specimens: interaction between the beam and column during moment transfer induced rotational movement and local compressive stresses in the connection region. However, the onset of buckling occurred at a later stage in the concrete-filled specimens compared to the hollow ones. This delay is attributed to the increased stiffness and confinement effect provided by the infilled concrete, which enhanced the local stability of the steel components and delayed the transition from elastic to plastic behaviour. Despite this improvement, the absence of bolted connections in the region where buckling developed, together with the insufficient thickness of the stiffening plates, caused the connection plates to lose elasticity and enter a plastic state. As a result, the beam again failed to achieve its full moment-carrying capacity, and no local buckling was observed in either the beam or the column. The failure mechanism was dominated by the local buckling and plastic deformation occurring at the connection, which hindered proper moment transfer and resulted in partial system failure. Although both specimen types of experienced connection failure due to local buckling, the delayed occurrence in the concrete-filled specimens indicates a superior energy absorption and ductility capacity characteristic of composite elements. The concrete infill increased the confinement of the steel section, thereby improving its resistance to local instability. Nevertheless, since the observed buckling occurred mainly in the connection region rather than along the beam itself, the connection configuration remained the weak point of the system. This suggests that the global performance of the structure was limited by the local instability of the joint region, rather than by the strength of the beam or column members. In summary, the experimental findings emphasize the necessity of improving connection stiffness, plate thickness, and bolt arrangement in order to delay or prevent local buckling and enhance moment transfer efficiency.

Although concrete-filled specimens demonstrated better performance through delayed buckling and improved stability, both connection types ultimately failed due to insufficient local strength in the connecting plates. Future designs should therefore focus on optimizing connection geometry and employing adequately stiffened connection plates to achieve higher moment-carrying capacity and greater structural resilience. Figs. 5(a) and 5(b) illustrate the failure modes observed in the connections of the hollow specimens after cyclic loading, showing the front and back faces, respectively. Figs. 5(c) and 5(d) present the corresponding failure modes for the concrete-filled specimens, also showing the front and back faces.

4. Conclusions

In this study, the connection between concrete-filled steel columns with stiffening plates and bolts and concrete-filled steel beams was investigated with theoretical studies and experimental tests. A total of two specimens were tested experimentally, one hollow test specimen and the other concrete-filled test specimen. Experimental results were compared with theoretical results obtained from code. The main results obtained from testing a limited number of test elements are listed below as so-called bullet points:

- Experimental data demonstrated that concrete-filled specimens had a significantly higher moment-carrying capacity compared to hollow specimens. This suggests that the concrete infill enhances the rigidity of

the connection components and encourages a more uniform stress distribution inside the cross-section. The concrete infill enhances stability in the connecting area by delaying local buckling.

- Upon comparing the theoretical analysis results with the results of the experiment, it was concluded that the investigated connection type can transmit a particular amount of moment; however, this transmission is inadequate for the design requirements. The connection geometry and weld specifications are believed to impose a constraint on the moment-carrying capacity.
- Moreover, it was determined that if the connection were utilized in its existing configuration, local buckling in the beam would occur in the connection region prior to the achievement of the beam's moment capacity. This suggests that the connection element demonstrates behaviour that may adversely impact its moment-bearing capacity and result in premature system failure. Consequently, it was determined that the connection specifications require enhancement, and supplementary measures must be implemented to augment the moment-carrying capability.

Future research seeks to duplicate the stiffening plate by increasing its size, modifying the concrete infill class, varying the steel cross-sections, varying the dimensions of the connection parts, varying the bolt class, and experimenting with other connection types.

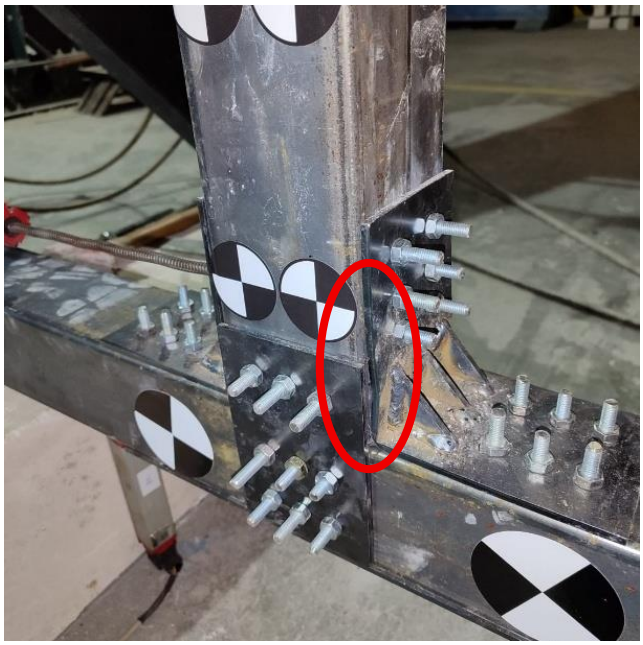

(a) Hollow connection (front)

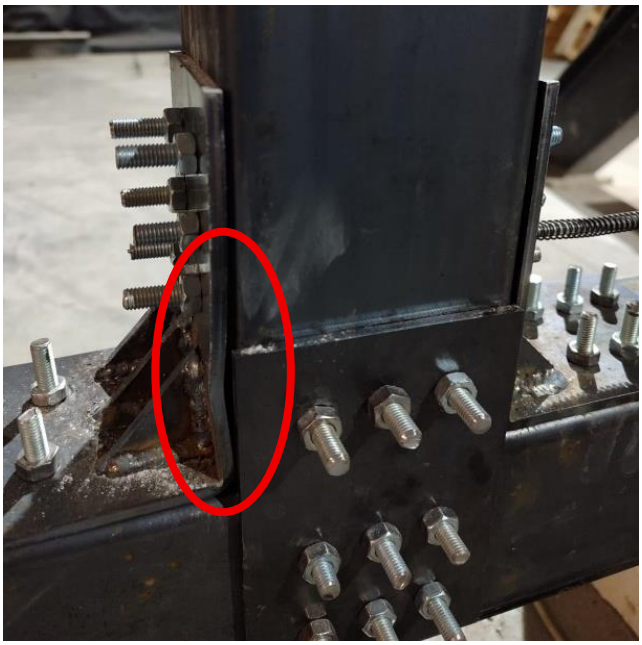

(b) Hollow connection (back)

(c) Concrete-filled connection (front)

(d) Concrete-filled connection (back)

Fig. 5. Failure modes in the connections of the hollow specimens after cyclic loading.

Acknowledgements

None declared.

Funding

This research was supported by Scientific Research Projects Commission of KTO Karatay University, Konya, Türkiye under grant number 10092430.

Conflict of Interest

The authors declared no potential conflicts of interest with respect to the research, authorship, and/or publication of this manuscript.

Author Contributions

All of the authors made substantial contributions to conception and design, or acquisition of data, or analysis and interpretation of data; were involved in drafting the manuscript or revising it critically for important intellectual content; and gave final approval of the version to be published.

Data Availability

The datasets created and/or analyzed during the current study are not publicly available, but are available from the corresponding author upon reasonable request.

REFERENCES

Abed FH, Abdelmageed YI, Ilgun A (2018). Flexural response of concrete-filled seamless steel tubes. *Journal of Constructional Steel Research*, 149, 53–63.

Al-Ani YR (2018). Finite element study to address the axial capacity of the circular concrete-filled steel tubular stub columns. *Thin-Walled Structures*, 126, 2–15.

Chen QJ, Cai J, Bradford MA, Liu X, Zuo ZL (2014). Seismic behaviour of a through-beam connection between concrete-filled steel tubular columns and reinforced concrete beams. *Engineering Structures*, 80, 24–39.

Chen Y, Feng R, Gong W (2018). Flexural behavior of concrete-filled aluminum alloy circular hollow section tubes. *Construction and Building Materials*, 165, 173–186.

FEMA-350 (2000). Recommended seismic design criteria for new steel moment-frame buildings. Federal Emergency Management Agency, Washington, DC, USA.

Han L-H, Lu H, Yao G-H, Liao F-Y (2006). Further study on the flexural behaviour of concrete-filled steel tubes. *Journal of Constructional Steel Research*, 62, 554–565.

Ibañez C, Hernández-Figueirido D, Piquer A (2018). Shape effect on axially loaded high strength CFST stub columns. *Journal of Constructional Steel Research*, 147, 247–256.

İlgün A, Sancıoğlu S (2023). Flexural behaviour of different CFSTs cross-section shapes with the same steel cross-sectional area. *Sādhanā*, 48, 53.

Kandil K, El-Shami M, Hekal G, ElGouhary O (2025). Behavior of multicell steel columns under impact loading. *Challenge Journal of Concrete Research Letters*, 16(2), 95-114.

Kazemzadeh Azad S, Li D, Uy B (2021). Compact and slender box concrete-filled stainless steel tubes under compression, bending, and combined loading. *Journal of Constructional Steel Research*, 184, 106813.

Liao JJ, Zeng JJ, Long YL, Cai J, Ouyang Y (2022). Behavior of square and rectangular concrete-filled steel tube (CFST) columns with horizontal reinforcing bars under eccentric compression. *Engineering Structures*, 271, 114899.

Lu YQ, Kennedy DJL (1994). The flexural behaviour of concrete-filled hollow structural sections. *Canadian Journal of Civil Engineering*, 21, 111–130.

Na L, Yiyan L, Shan L, Lan L (2018). Slenderness effects on concrete-filled steel tube columns confined with CFRP. *Journal of Constructional Steel Research*, 143, 110–118.

Nakanishi K, Kitada T, Nakai H (1999). Experimental study on ultimate strength and ductility of concrete filled steel columns under strong earthquake. *Journal of Constructional Steel Research*, 51, 297–319.

Özkılıç YO (2023). Cyclic and monotonic performance of unstiffened extended endplate connections having thin end-plates and large-bolts. *Engineering Structures*, 281, 115794.

Qu X, Xie Y, Sun G, Liu Q, Wang H (2023). Seismic behavior of assembly joint with CFST column and H-shaped steel beam. *KSCE Journal of Civil Engineering*, 27(2), 670–683.

Sancıoğlu S (2025). Experimental Investigation on Moment Carrying Capacity of Column – Beam Connections Consisting of Concrete-Filled Steel Composite Members. *Ph.D thesis*, KTO Karatay University, Konya, Türkiye.

Schneider SP (1998). Axially loaded concrete-filled steel tubes. *Journal of Structural Engineering*, 24, 1125–1138.

Solak K, Orhan S (2023). Axial compression behaviour of concrete-filled auxetic tubular short columns. *Challenge Journal of Concrete Research Letters*, 14(1), 1-9.

TS 802 (2016). Calculation principles of concrete mix design. Turkish Standards Institute, Ankara, Türkiye.

TS EN 12390-3 (2019). Testing hardened concrete – Part 3: Compressive strength of test specimens. Turkish Standards Institute, Ankara, Türkiye.

TS EN ISO 6892-1 (2020). Metallic materials – Tensile testing – Part 1: Method of test at room temperature. Turkish Standards Institute, Ankara, Türkiye.

Turkish Steel Structures Regulation (2018). Principles of design, calculation, and construction of steel structures. Republic of Türkiye Ministry of Environment, Urbanization, and Climate Change, Ankara, Türkiye.

Urtekin Y, Çelik Z (2025). Investigation of the effects of re-curing on mechanical properties of basalt-polypropylene hybrid fiber concretes after exposure to high temperature. *Challenge Journal of Structural Mechanics*, 11(1), 14-23.

Wang JF, Han LH, Uy B (2009). Hysteretic behaviour of flush end plate joints to concrete-filled steel tubular columns. *Journal of Constructional Steel Research*, 65, 1644–1663.

Ye Q, Wang Y, Wang Z, Lin Y, Shu C, Zhang F (2021). Experimental study of through diaphragm bolted joint between H-beam to CFST column. *Journal of Constructional Steel Research*, 182, 106647.

Yıldız Y, Şermet F (2025). Impact of composite columns on soft and weak storey irregularities in buildings without ground floor infill walls. *Challenge Journal of Structural Mechanics*, 11(2), 70-81.